Biomedicine & Pharmacotherapy 150 (2022) 112979

Contents lists available at ScienceDirect

Biomedicine & Pharmacotherapy

journal homepage: www.elsevier.com/locate/biopha

Assessment of therapeutic effect of CD20-targeted immunoliposome in primary central nervous system lymphoma

Nutthanit Thumrongsiri [a], Paweena Dana [a], Rand Bawab [b], Prattana Tanyapanyachon [a], Chaichana Treetidnipa [c], Nattika Saengkrit [a,*], Sith Sathornsumetee [c,d,**]

[a] National Nanotechnology Center (NANOTEC), National Science and Technology Development Agency (NSTDA), Pathumthani 12120, Thailand
[b] Department of Biomedical Engineering, University of Victoria, Victoria, BC V8W 2Y2, Canada
[c] Research Network NANOTEC-Mahidol University in Theranostic Nanomedicine, Faculty of Medicine Siriraj Hospital, Mahidol University 2 Wanglang Road, Bangkoknoi, Bangkok 10700, Thailand
[d] Department of Medicine (Neurology), Faculty of Medicine Siriraj Hospital, Mahidol University 2 Wanglang Road, Bangkoknoi, Bangkok 10700, Thailand

ARTICLE INFO

Keywords:
Lymphoma
CNS
CD20
liposome
rituximab
nanoparticle

ABSTRACT

Primary central nervous system lymphoma (PCNSL) is a form of extranodal non-Hodgkin's B-cell lymphoma limited to the CNS. The treatment of PCNSL is ineffective partly due to the blood-brain barrier (BBB) restriction of delivery of many drugs including anti-CD20 (Rituximab; RTX) which is a standard treatment for systemic B-cell lymphomas. In this study, liposome with tween-80 surface modification was fabricated and conjugated with RTX for enhancing BBB penetration to target lymphoma cells in the CNS. Physicochemical characterizations of Lip/RTX were performed and spherical shape liposomes with narrow size distribution were demonstrated by TEM. An average diameter of Lip/RTX was 168.57 ± 1.57 nm with the percentage of RTX conjugation at 90.94. Cell internalization monitored by flow cytometry confirmed that conjugation of RTX promoted liposome entry into Raji cells expressing CD20. Antitumor activity of Lip/RTX was comparable to free RTX indicating that RTX moieties on liposome remained their therapeutic function. In addition, Lip/RTX inhibited tumor aggressiveness by limiting cell migration and invasion. Systemic administration of Lip/RTX significantly prolonged survival of mice harboring intracranial lymphoma xenografts. Taken together, Lip/RTX presents a new potential treatment for patients with PCNSL.

1. Introduction

Primary central nervous system lymphoma (PCNSL) is an aggressive lymphoma of the central nervous system (CNS) which is known as an extranodal non-Hodgkin lymphoma. PCNSL is commonly restricted to brain, eyes, spinal cord, leptomeninges and cerebrospinal fluid (CSF), with an absence of systemic spread [15,21,23]. PCNSL is a rare tumor since it accounts for only 3 – 6% of all brain tumors [23]. However, the incidence has recently increased, particularly in immunocompromised patients, whom are at higher risk of developing PCNSL than immunocompetent patients [21]. Moreover, the incidence of PCNSL has risen in elderly population with a rate of 0.5 per 100,000 per year [7,15]. In addition, PCNSL also affects transplant patients who received immunosuppressive therapy [32,39].

Intravenous high dose methotrexate (HD-MTX)-based regimen is the primary treatment for most patients with PCNSL. Other chemotherapies such as cytarabine, ifosfamide, procarbazine, vincristine and temozolomide have been combined with HD-MTX [6,24,33]. However, many of these agents hardly reach PCNSL since they scarcely pass through the blood-brain barrier (BBB) [25]. BBB is recognized as a highly selective biological barrier that is formed by a unique tight junction of capillary endothelial cells, pericytes and astrocytes [1,20]. One of the BBB functions is to limit the entrance of potential toxic substances including drugs and large molecules to the CNS [11,27,35]. Therefore, the development of delivery system that facilitates drug penetration across the BBB is a promising strategy to improve therapeutic outcome of CNS cancers including PCNSL.

Among several pharmaceutical delivery systems, nanotechnology

* Corresponding author.
** Corresponding author at: Research Network NANOTEC-Mahidol University in Theranostic Nanomedicine, Faculty of Medicine Siriraj Hospital, Mahidol University 2 Wanglang Road, Bangkoknoi, Bangkok 10700, Thailand.
E-mail addresses: nattika@nanotec.or.th (N. Saengkrit), sith.sat@mahidol.edu (S. Sathornsumetee).

https://doi.org/10.1016/j.biopha.2022.112979
Received 15 February 2022; Received in revised form 8 April 2022; Accepted 14 April 2022
Available online 20 April 2022

has been exploited to improve the transportation of drugs across the BBB. Nano-drug delivery systems improve the specific binding of drug to target cells and prolong the drug's bioavailability [8,28]. Liposome is a synthetic phospholipid bilayer vesicle which facilitates the combination loading of hydrophilic and hydrophobic drugs. The hydrophilic drugs are entrapped within the core of liposome while hydrophobic drugs are loaded in a bilayer membrane. Liposomal drug delivery system has been employed for brain tumor treatments, for example, the multifunctional liposome constructed with cyclic RGD (RGD: arginine-glycine-aspartic) and p-hydroxybenzoic acid (pHA) targeting glioma. The cyclic RGD was loaded at the surface of liposome to promote the binding of liposome to integrin, which is highly expressed on glioma cells, whereas pHA binds to dopamine receptor of the BBB [3].

Rituximab (RTX) is an anti-CD20 monoclonal antibody, which has been approved for treatment of B-cell lymphomas [6,26,29]. Although RTX is an effective therapeutic antibody against systemic lymphoma, the efficacy in PCNSL is limited because of the delivery restriction by the BBB [2]. Hence, the strategy to improve the transport of RTX across the BBB is needed. Our previous study demonstrated that RTX conjugated with liposomal-SPION permeated through the in vitro model of BBB better than unconjugated RTX [30]. In order to advance therapeutic agent into clinical trial evaluation, we here simplified the formulation of liposomal RTX without SPION loading. In the present study, we aimed to evaluate the therapeutic efficacy of RTX-conjugated liposome without SPION in both in vitro experiments and in vivo surviva ml study following systemic administration in mice bearing intracranial lymphoma xenografts.

2. Materials and methods

2.1. Materials

Soybean lecithin (Soya phosphatidylcholine; PC) was purchased from American Lecithin Co, Danbury, CT. 1,2-Distearoylsn-glycero-phosphoethanolamine-N-[amino(polythyleneglycol 2000)] (DSPEG-PE) and 1,2-dioleoyl-sn-glycero-3-phosphoethanolamine-N-[4-(p maleimidophenyl)butyramide](MPB-PE; linker) were purchased from Avanti Polar Lipids, Inc (Alabama, USA). Polysorbate80 (Tween 80) was obtained from Sigma-Aldrich (Saint Louis, MO, USA). Phosphate buffered saline (pH 7.4) (PBS; containing 137 mM NaCl, 2.7 mM KCl, 10 mM Na_2HPO_4; 2 mM KH_2PO_4) was from Gibco (Paiseley, UK). TritonX-100 was obtained from Merck (Merck Millipore, Darmstadt, Germany). Anti-CD20 (RTX) was purchased from Roche (Basel, Switzerland). Media (Roswell Park Memorial Institute Medium; RPMI 1640, Dulbecco's Modified Eagle Medium; DMEM) and supplements (Fetal bovine serum; FBS, 0.25% Trypsin EDTA, penicillin G sodium, streptomycin) were purchased from GIBCO Invitrogen (New York, USA). MTT [3-(4,5-Dimethylthiazol-2-yl)− 2,5-diphenyltetrazolium bromide] was purchased from Merck (Darmstadt, Germany). Distilled water was generated using an ELGA system (PureLab Ultra, Illinois, USA). Matrigel was acquired from Corning (Massachusetts, USA). For gelatin zymography, gelatin, tris, sodium azide (NaN_3), glycine and Triton X-100 were ordered from Sigma (Missouri, USA). Sodium dodecyl sulphate (SDS), zinc chloride ($ZnCl_2$) and calcium chloride ($CaCl_2$) were from Merck (Darmstadt, Germany). 30%crylamide-0.8%bis acrylamide, TEMED, Coomassie blue G250 and ammonium persulfate were from BioRad (California, USA). Ethanol, hydrochloric acid (HCl) and acetic acid were obtained from RCI labscan (Bangkok, Thailand).

2.2. Methods

2.2.1. Liposome formulation and characterization

Liposome formulation was based on thin-film hydration method. In brief, PC, Tween 80, DSPEG-PE and MPB-PE (linker) (10: 1.25: 0.1:0.01 wt ratio, respectively) were prepared and dissolved in diethyl ether. Then, solvent was removed by rotary evaporator. Lipid film was hydrated with PBS buffer (pH 7.4), reduced the vesicles size by using 200 nm pore size of polypropylene membrane (Millipore GmbH, Eschborn, Germany) through extruder with 15–20 cycles. Thiolated RTX was prepared by mixing RTX with 2-iminothiolane at room temperature for 1 h, subsequently added to liposome and stirred continuously at 4 °C overnight in order to obtain the conjugated liposome (Lip/RTX). The excess residues were removed by ultra-centrifugal at 80000 rpm for 1–2 h. The investigation of size and zeta potential of liposome was performed using dynamic light scattering (DLS Ultra, Malvern Instruments, Malvern, UK) and morphology of liposome was observed under transmission electron microscopy (TEM) (JEM 2100 plus, JEOL, USA).

2.2.2. Cell culture and cell viability assay

Raji cell line was cultured in RPMI1640 supplemented with 10% FBS, 1% L-Glutamine (100 g/ml L-glutamine) plus 1% antibiotics (100 g/ml streptomycin and 100 U/ml penicillin). Cells were cultivated at 37 °C under humidified atmosphere containing 5% of CO_2 until reaching 70–80% cell confluence. To evaluate cell viability following exposure with conjugated liposome, Raji cell at a density of 5×10^4 cells were seeded in 96 well-plate and incubated for 24 h. Each well was exposed to liposome according to phospholipid concentration starting at 200 μg/ml as a final concentration followed by 10-fold dilution with PBS buffer for 7 subsequent dilutions. Treated cells were further cultivated for 24 h and then treated with MTT solution (5 mg/ml) for 4 h. The solution of 0.04 N hydrochloric in isopropanol v/v was used in order to dissolve crystal formazan followed by absorbance measurement at 570 nm using microplate reader (SpectroMAX, California, US).

2.2.3. Cellular internalization

Raji cells were cultured as previously described, seeded into 24 well-plate (1×10^5 cells), and incubated overnight. Liposome and conjugated liposome stained with dil dye at a ratio of 1:1000 v/v were subsequently added to cells in triplicate, at the concentration of IC80 acquired from cell viability assay. Cells were collected at 0, 0.5 and 1 h after incubation. Prior to measurement, unbound particles were removed from cells with PBS buffer for three times. Internalization signal intensities in each exposure time were analyzed using flow cytometer (BD FACS CaliburTM, BD biosciences, CA, USA) with excitation and emission wavelengths of 488 nm and 600 nm, respectively.

2.2.4. Cell invasion and migration

In order to evaluate cell invasion, the 6.5 mm transwell together with 8.0 μM pore size polycarbonate membrane insert was coated with Matrigel at concentration of 0.4 mg/ml prior to cell seeding. For cell migration assay, cells can be seeded directly to the transwell. Raji cells at a density of 1×10^5 cells were suspended in serum-free medium and seeded into transwell. Lip/RTX was added with IC20 concentration of RTX at 80 μg/ml. Cells were then incubated for 5 and 6 h to assess cell migration and cell invasion, respectively. The upper chambers were removed and cells that escaped from the upper compartment were stained with Hoechst and observed under optical fluorescence microscope.

2.2.5. Gelatin zymography

Raji cells at a density of 1×10^6 cells were seeded into 48 well-plate and cultured for 24 h. The cells were treated with liposome nanoparticles at RTX 80 μg/ml, then, incubated overnight in previously described conditions. Cells were collected, centrifuged, re-suspended in serum-free medium, and incubated for 24 h. Then, the supernatants were collected to undergo gelatin zymography that was performed on sodium dodecyl sulfate polyacrylamide gel electrophoresis (SDS-PAGE) in which the co-polymerization of acrylamide and gelatin were employed for gel setting. The separating SDS gel consisted of 0.1% (w/v) gelatin solution, 375 mM Tris-HCl pH8.8, 10% (w/v) of acrylamide:bis-acrylamide (37.5: 1), 0.4% (v/v) glycerol, 0.1% (w/v) SDS, 0.05% (v/v) TEMED and 0.1% (w/v) ammonium persulphate (APS). Stacking gel

contained 4% (w/v) acrylamide:bis-acrylamide (37.5: 1), 0.12 M Tris-HCl pH6.8, 0.1% (w/v) SDS, 0.23% (v/v) TEMED and 0.08% (w/v) APS. Running buffer during the separation consisted of 0.1% SDS and Tris-glycine buffer (25 mM Tris and 192 mM glycine). The running condition was under constant voltage of 100–110 V for stacking phase and 150–200 V for running phase. Staining procedure was performed by immersing the gel in denaturing buffer (2.5% Triton X-100 in 50 mM Tris-HCl pH7.4, 5 mM $CaCl_2$, 1 μM $ZnCl_2$ and 0.01% NaN_3), then, gently shaken for 1 h, replaced with developing buffer (50 mM Tris-HCl pH7.4, 5 mM $CaCl_2$, 1 μM $ZnCl_2$ and 0.01% NaN_3) and finally incubated overnight at 37°C. Gel was subsequently stained in 0.5% Coomassie blue G250 in 30% ethanol and 10% acetic acid for 30 min. Gel was washed and backgrounded with de-staining solution (30% ethanol and 10% acetic acid) until the clear band could be observed. The washing process was stopped by adding 0.2% acetic acid solution.

2.2.6. *In vivo survival study*

Nude mice (NOD) were obtained from the Central Institute of Experimental Animal; CIEA Japan. Mice were housed and monitored in the Laboratory Animal Research and Case Center, Siriraj hospital (Mahidol University, Thailand) according to institutional guidelines. All experimental procedures and protocols were performed by S.S. and C.T. The study was approved by the Laboratory Animal Research and Case Center, Siriraj hospital, Mahidol University, Thailand under animal care with protocol no. 001/2558.

To induce xenograft of PCNSL in mice, female nude mice (4–6 weeks) were intracranially injected with Raji cells at a cell density of 5×10^4 cells in volume of 20 μL in RPMI medium [30]. Seven days after implantation, the mice were divided into three groups (N = 4 each group) to investigate the therapeutic effect of free RTX, Lip/RTX and PBS. The mice were intravenously injected with 50–100 μL of free RTX, Lip/RTX or PBS via tail injection once weekly for 3 months. Food and water were provided ad libitum. The survival study was investigated under guidelines of humane endpoints in animal study procedure including lethargy, loss of locomotor activity and weight loss (up to 25%). The survival time of the mice was calculated from the day of lymphoma cells inoculation to the day of euthanasia or death. The median survival time of mice was calculated and Log-rank test was used to compared survival among groups (GraphPad Prism 8, USA).

3. Results and discussion

3.1. *Physiochemical characterization of liposome*

The average size, polydispersity index (PDI), and zeta potential of the liposomes were measured by dynamic light scattering (DLS) using Zetasizer. The average diameters of formulated liposomes, Lip/- (unconjugated liposome) and Lip/RTX, were 163.93 ± 2.59 nm and 168.57 ± 1.57 nm, respectively (Table 1). This result indicated that conjugation of RTX with liposome did not significantly induce diameter change. The zeta potential of Lip/- was − 1.11 ± 0.24 mV, which was in line with our previous data [30]. Our liposome formulation possessed slightly lower negative charge on the surface. For the conjugated liposome, Lip/RTX, the zeta potential was − 0.11 ± 0.19 mV, which was slightly more positive when compared with Lip/-. The fluctuation of liposomal surface charge was likely related to the charge of conjugated RTX as similarly occurred in other studies [19,22]. The monodispersed characteristics of the liposomes were confirmed from the PDI value of Lip/- and Lip/RTX of 0.09 ± 0.01 and 0.10 ± 0.00, respectively [10].

Table 1
Size, zeta potential, polydispersity index (PDI) and RTX conjugation percentage of Lip/- and Lip/RTX.

Sample	Size (nm)	Zeta potential (mv)	PDI	%Conjugation of RTX	Phospholipid (mg/ml)
Lip/-	163.93 ± 2.59	-1.11 ± 0.24	0.09 ± 0.01	–	12.12
Lip/RTX	168.57 ± 1.57	-0.11 ± 0.19	0.10 ± 0.00	90.94	13.51

The morphological characteristics of Lip/- and Lip/RTX were observed under TEM. TEM images confirmed the spherical vesicles of nanoparticles as shown in Fig. 1. The morphologies of the liposomes, including shape and size, are important in terms of function and drug release properties. The spherical shape and uniformed size exhibit the resemblance of drug release patterns and prolonged shelf-life stability [5,8]. As suggested by several studies, the optimal nanoparticle size range between 70 and 200 nm since larger nanoparticles are rapidly cleared by opsonization [13]. Taken together, our fabricated liposomes satisfied the nanoparticle criteria to be used as a drug delivery system.

3.2. *Quantification of RTX conjugation onto liposome*

The percentage of RTX conjugated onto liposome was calculated via an indirect approach. Unbound RTX was determined using Micro BCA™ Protein assay kit (Thermo Scientific, Rockford, USA). The result was then subtracted by the amount of loaded RTX. As a result, approximately 90% of loaded RTX was successfully conjugated onto liposome (Table 1). Phospholipid concentration was analyzed to evaluate the lipid content using Lab assay phospholipid C Kit (Fujifilm, Osaka, Japan). The lipid contents of Lip/- and Lip/RTX were 12.12 and 13.51 mg/ml, respectively (Table 1). The obtained data were employed to quantify liposome for investigating cytotoxicity and cellular uptake.

3.3. *Cellular internalization*

The therapeutic efficacy of targeted liposome depended on the internalization ability into the target cell. In this study, RTX acted as not only a therapeutic antibody, but also a moiety to bind to CD20 receptor. Since CD20 receptors are located on the surface of mature B-cells and most B-cell lymphomas including PCNSL [26,29,37], we evaluated cellular uptake of our liposomes in CD20 expressed Raji cells that are commonly exploited in preclinical studies of PCNSL. Raji cells were incubated with FITC encapsulated Lip/- and Lip/RTX at IC20 concentration. All samples were incubated at 0, 0.5 and 1 h. The signal intensities were quantified by flow cytometry and analyzed by FlowJo software 10.5.3. As shown in Figs. 2a and 2b, Lip/RTX was able to enter Raji cells faster than LIP/-, which indicated that RTX conjugation facilitated liposome internalization. The signal intensities were quantified and calculated to display statistically significant difference ($P < 0.001$) between Lip/- and Lip/RTX (Fig. 2**c**). Since the successful entry of liposome depended on its physicochemical property, the internalization could not be elevated without RTX even after excessive incubation time. Based on the presence of CD20 receptors on Raji cell surface, it is irrefutable that incorporation of RTX ligand successfully enhanced cell internalization.

3.4. *Therapeutic effect of Lip/RTX on lymphoma cells*

Therapeutic effect of Lip/RTX was assessed by MTT assay with Raji suspension cells. Two approaches were examined to evaluate Lip/RTX effect on Raji cells. First, two-folds dilution samples with varied concentration of RTX from 0 to 400 μg/ml were incubated with Raji cells for 24 h to investigate the function of RTX attached on liposome compared with free RTX. The result shown in Fig. 3a indicated that free RTX and Lip/RTX exhibited the comparable activity meaning that the function of conjugated RTX remained equivalent to free RTX. The attachment of RTX on liposomes did not promote the RTX function via cellular uptake. This may be due to the binding mechanism of RTX in killing cancer cells. RTX binds to the FcγRIIIa receptor indulging the antibody-dependent

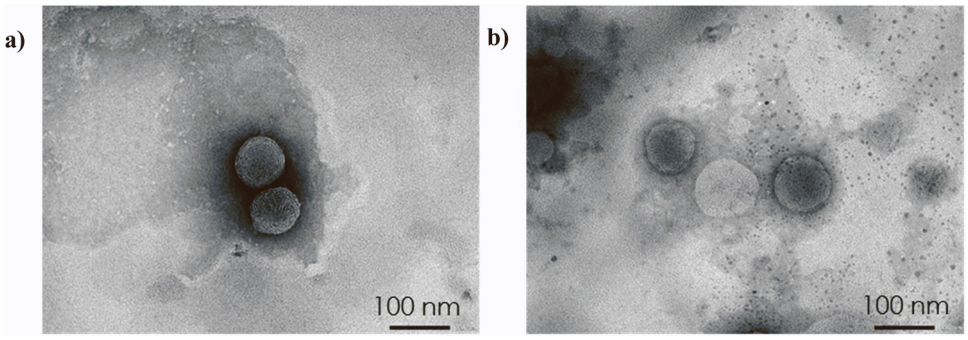

Fig. 1. TEM image of Lip/- (a) and Lip/RTX (b). The images were monitored by TEM at 120 kV and 80000x magnification level. The100 nm scale bar was indicated at the bottom right of each image.

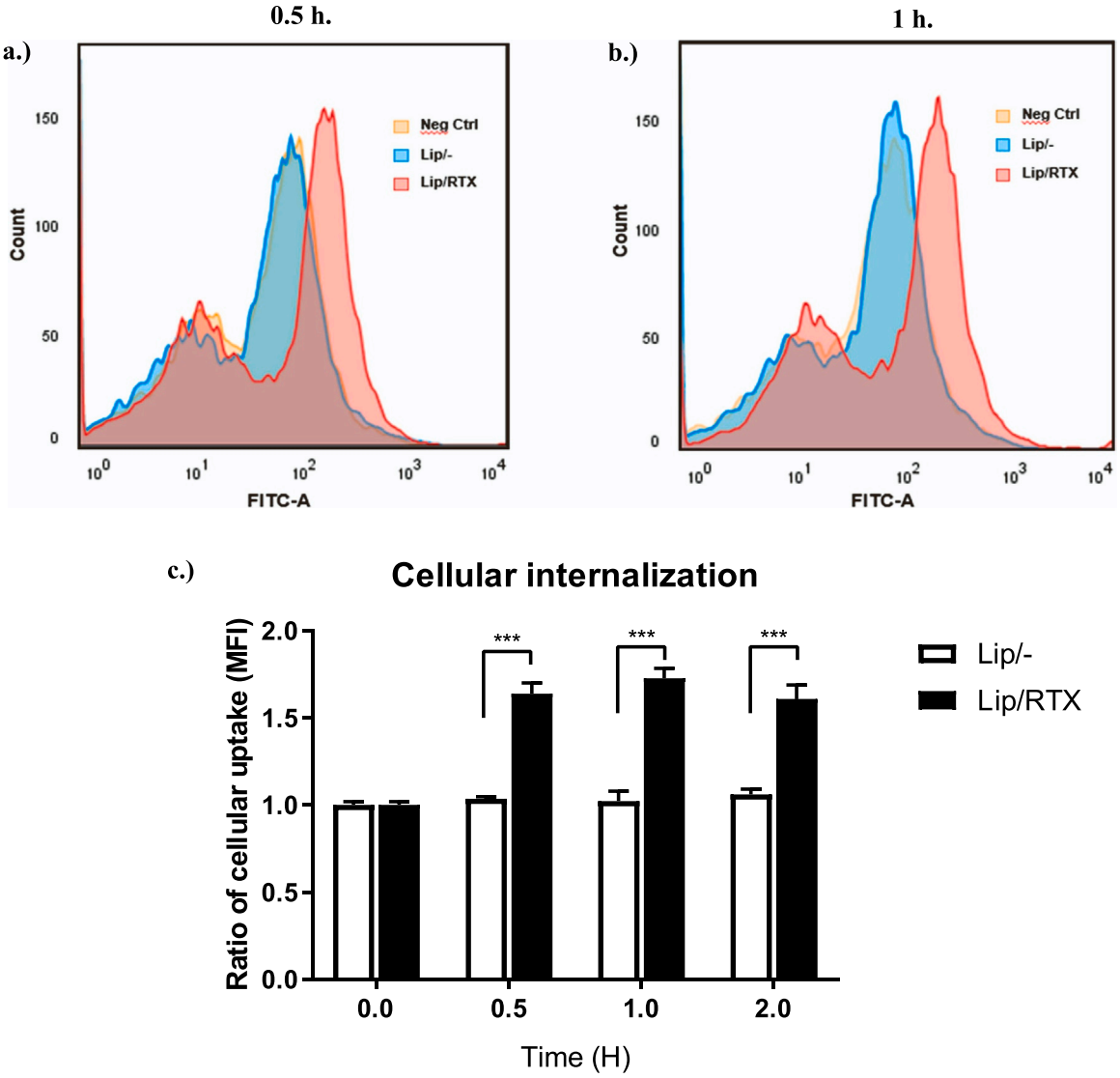

Fig. 2. Lip/RTX internalization in Raji cell comparing with Lip/-. The signal intensity was quantified by flow cytometry. Liposome samples were stained by dil dye and incubated in Raji cell for 0.0, 0.5, 1.0 and 2.0 h. a.) & b.) Histograms indicated the mean fluorescence intensity of liposome samples uptake by Raji cells at 0.5 h (a.) and 1 h (b.). c.) Quantitative ratio of cellular uptake calculated from mean intensity at * **$p < 0.001$.

cell-mediated cytotoxicity (ADCC) response [4,12]. Therefore, the cell entry pathway of both Lip/RTX and free RTX operated on RTX as a targeting ligand which provided the same function as a therapeutic antibody. Furthermore, the percentage of cell viability was observed to examine therapeutic effect of Lip/RTX and compared with unconjugated liposome, Lip/-. The lipid contents of Lip/- and Lip/RTX were varied in 10 folds dilution ranging from 2×10^{-4} to 2×10^{2} μg/ml to treat Raji cells for 24 h. The unconjugated liposome did not display cell toxicity traits in Raji cells as the viability was higher than 80%. In contrast, RTX conjugated liposome could induce cell toxicity in a dose-dependent

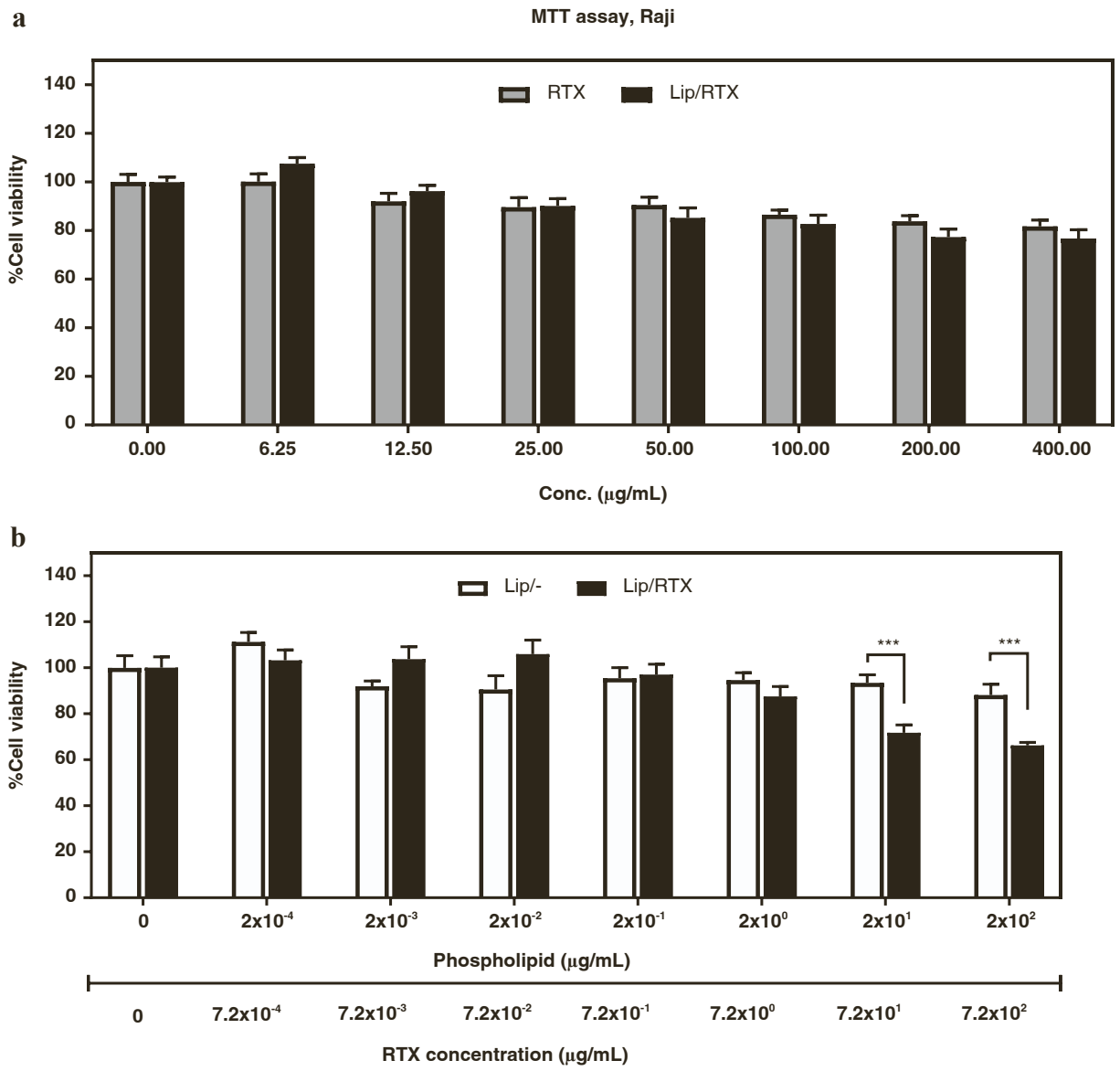

Fig. 3. a Percentage of Raji cell viability determined by MTT assay post-incubation of free RTX (gray bar) and Lip/RTX (black bar) for 24 h. The assay was done at the varied RTX concentration ranging from 0 to 400 μg/ml.Fig. 3b. Examination of therapeutic effect of Lip/RTX compared to Lip/-. The data presented cell viability evaluation from MTT assay. Raji cells were exposed to Lip/- and Lip/RTX at different phospholipid concentrations from 0 to 2×10^2 μg/ml for 24 h. White bars represent Lip/- while black bars represent Lip/RTX.

manner. The significant differences (***$P < 0.001$) were evaluated in the higher concentrations of lipid content (2×10^1 to 2×10^2 μg/ml, which were equal to RTX concentration of 72 μg/ml to 720 μg/ml, respectively), where the cell viability remained less than 80% (Fig. 3b). This result indicated that Lip/RTX could disturb lymphoma cell survival rate at the concentration of RTX greater than 72 μg/ml.

3.5. Inhibition of tumor aggressiveness by Lip/RTX

Inhibition of tumor aggressiveness by Lip/RTX was examined and compared with the free-RTX using cell migration an invasion assay. The migrated cells in the lower compartment were stained to be observed under microscope and quantified (Fig. 4). Both free RTX and Lip/RTX significantly limited migration and invasion of Raji cells from upper to lower chambers. The activity of RTX against cell migration/invasion was not affected by the liposome conjugation.

3.6. Determination of gelatinase activity in Raji cells

Gelatinases such as matrix metalloproteinase 2 (MMP-2) and matrix metalloproteinase 9 (MMP-9) are essential in migration and invasion of cancer cells in a metastatic pathway. These proteins degrade extracellular matrix as a prerequisite for cancer cell invasion giving rise to metastases [36,38]. High expression of MMP-9 but not MMP-2 correlated with aggressiveness and poor survival in patients with B-cell lymphoma [31]. We demonstrated that rituximab (both free and liposome-conjugated) reduced aggressive phenotypes (migration and invasion) of lymphoma cells (Fig. 4). We hypothesized that downregulation of gelatinases, particularly MMP-9, in lymphoma cells might represent a mechanism of rituximab-mediated inhibition of cell migration/invasion as rituximab was also shown to downregulate MMP-9 in serum and lymphocytes from patients with rheumatoid arthritis [16,34]. Therefore, the gelatinase activity assay was performed. The gelatin embedded in a polyacrylamide gel exposed the activity of secreted MMP-9 and MMP-2 gelatinase enzymes as clear bands distinct from the

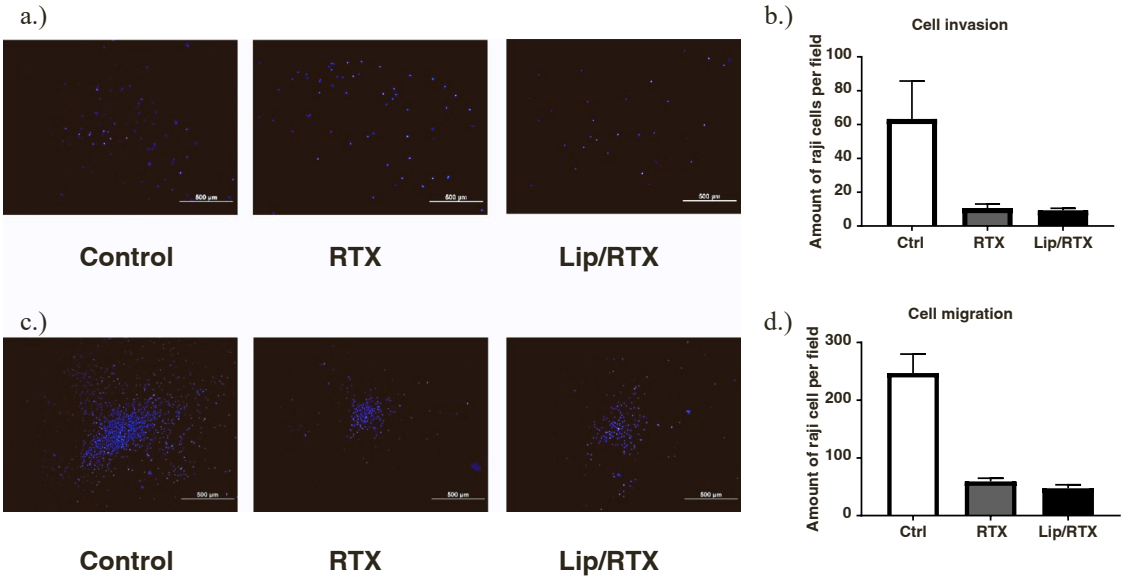

Fig. 4. Cell invasion and migration analysis. Raji lymphoma cells were treated with RTX and Lip/RTX for 6 h at a RTX concentration of 80 μg/ml. Cells in lower chamber were stained with Hoechst and observed under optical fluorescence microscope at 40x magnification. The scale bars of 500 μm were indicated. a.) Cell invasion b.) Cell migration c.) Quantitative signal of cell invasion and d.) Quantitative signal of cell migration.

background after Coomassie blue staining. The degradation signal of MMP-9 derived from Lip/RTX was lower than those from control and free RTX. (Fig. 5). The mechanism of reduction of MMP-9 activity in Lip/RTX more than free RTX was unclear but a plausible explanation may be that Lip/RTX was associated with greater cell internationalization than free RTX rendering higher inhibition of MMP-9 activity.

The MMP-2 signals were similar in control, free RTX and Lip/RTX, which was in line with previous studies [16,34]. Owing to the ability to cross BBB and the anti-lymphoma activities of Lip/RTX as shown in the in vitro studies, we then performed an in vivo study to evaluate therapeutic efficacy of Lip/RTX in mice bearing intracranial human lymphoma xenografts.

3.7. *In vivo study using mice bearing intracranial lymphoma xenografts*

In vivo study was performed to demonstrate the effect of targeted liposome, Lip/RTX, on the survival of mice bearing intracranial lymphoma xenografts. The PCNSL xenograft model was established in mice (N = 12) via intracranial injection of Raji cells. The survival times of mice with PCSNL were measured after systemic (tail vein injection) administration of PBS (N = 4), free RTX (N = 4), or Lip/RTX (N = 4) injection (Fig. 6). The median survival times were 7, 19 and 61 days for PBS, free RTX and Lip/RTX, respectively. Treatment with Lip/RTX was associated with significant survival benefit when compared to PBS or free RTX (log-rank $P < 0.0021$). This result confirmed the benefit of Lip/RTX over free RTX in a mouse model of PCNSL. In this study, tween80-containing liposome was rendered as a nanocarrier to overcome the limitation of RTX delivery across BBB. As supported by other studies, incorporation of tween80 in nanoparticle composites promotes BBB penetration though the binding of tween80 and receptor on astrocytes [9,14]. After injection, tween 80 containing liposomes were adsorbed onto the astrocyte through the binding of apolipoprotein E (apo E) [17] and interacted with low-density lipoprotein (LDL) receptor which then resulted in endocytosis of liposome into the cell [18].

In addition, the incorporation of PEG could reduce the mononuclear phagocyte system (MPS) uptake and decrease liposome and hydrophobic interaction in blood. By this approach, bioavailability of drug would be enhanced ([14]). Taken together, our Lip/RTX formulation successfully enhanced blood brain barrier penetration of RTX which intensifies the therapeutic efficacy allowing the mice bearing PCNSL to survive longer.

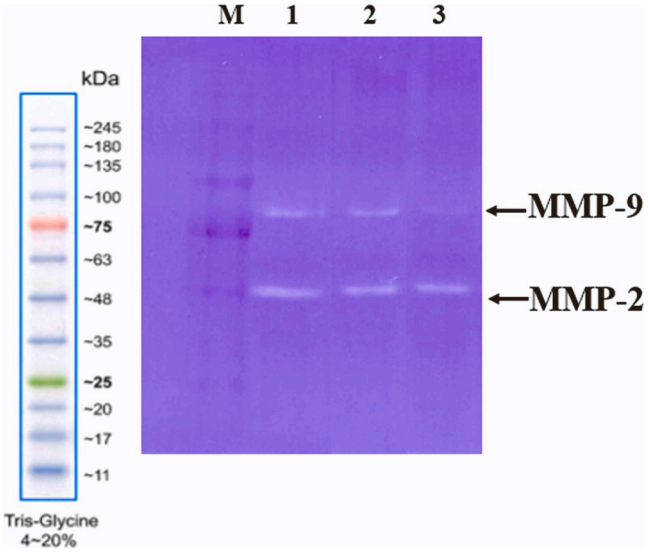

Fig. 5. Gelatinase activity analysis on SDS-PAGE from Raji cell condition media at 24 h. M = Marker, 1 = Control, 2 = RTX and 3 = Lip/RTX.

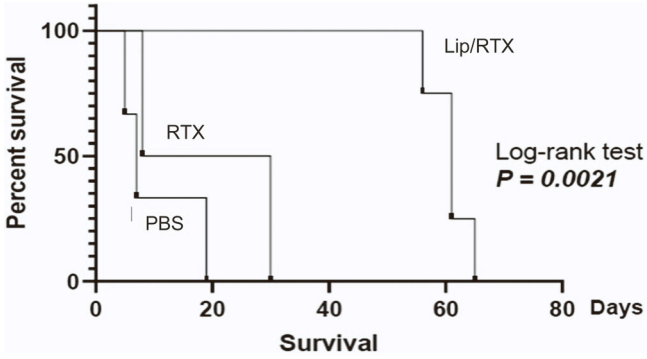

Fig. 6. Survival of mice bearing intracranial lymphoma xenografts after systemic administration of PBS, free RTX and Lip/RTX.

4. Conclusion

Our study demonstrated that the liposome-conjugated RTX was associated with greater survival benefit than free RTX in mice bearing intracranial lymphoma. The ligand-targeted liposome was composed of the principal component of the lipid bilayer alongside Tween 80 for steric stabilization and elasticity to cross the BBB. MPB-PE on the surface of liposome enabled the conjugation of antibodies or peptides and the liposome. In this case, PE-PEG improved liposome stability in blood circulation and the anti-CD20, RTX, on the surface led to the enhancement of cell targeting and therapeutic efficacy. This liposomal nano-delivery system is prospected to improve the drug transportation for treatment of not only PCNSL but also other neurologic disorders such as neurodegenerative diseases and autoimmune neurologic disorders.

CRediT authorship contribution statement

Nutthanit Thumrongsiri: Literature review, Design of research tools, Analysis of data, Interpretation of data analysis, Drafting of the article (first draft) **Paweena Dana:** Design of research tools, Analysis of data, Drafting of the article (first draft), Revising draft of the article (second draft) **Rand Bawab:** Design of research tools, Analysis of data **Prattana Tanyapanyachon:** Design of research tools, Analysis of data **Chaichana Treetidnipa:** Design of research tools **Nattika Saengkrit:** Conception of the project, Design of the research outline, Interpretation of data analysis, Final approval of the article (final draft) **Sith Sathornsumetee:** Conception of the project, Design of the research outline, Interpretation of data analysis, Final approval of the article (final draft).

Conflict of interest statement

There are no conflicts to declare.

Acknowledgements

This work was supported by the National Science and Technology Development Agency (NPT-RNN) (Grant no. P1851732) and National Research Council of Thailand (NRCT) (Grant no. N41A640102) to Saengkrit N. This work has been partially supported by the Research Network NANOTEC (RNN) program of the National Nanotechnology Center (NANOTEC), NSTDA, Ministry of Higher Education, Science, Research and Innovation (MHESI), Thailand and Siriraj Research Fund, Grant number R016141027, Faculty of Medicine Siriraj Hospital, Mahidol University to Sathornsumetee S.

References

[1] S. Bagchi, T. Chhibber, B. Lahooti, A. Verma, V. Borse, R.D. Jayant, In-vitro blood-brain barrier models for drug screening and permeation studies: an overview . Drug Des., Dev. Ther. 13 (2019) 3591–3605, https://doi.org/10.2147/DDDT.S218708.

[2] T.T. Batchelor, S.A. Grossman, T. Mikkelsen, X. Ye, S. Desideri, G.J. Lesser, Rituximab monotherapy for patients with recurrent primary cns lymphoma, Neurology 76 (10) (2011) 929–930, https://doi.org/10.1212/WNL.0b013e31820f2d94.

[3] Z. Belhadj, C. Zhan, M. Ying, X. Wei, C. Xie, Z. Yan, W. Lu, Multifunctional targeted liposomal drug delivery for efficient glioblastoma treatment, Oncotarget 8 (40) (2017) 66889–66900, https://doi.org/10.18632/oncotarget.17976.

[4] C. Bezombes, J.J. Fournié, G. Laurent, Direct Effect of Rituximab In B-cell-derived Lymphoid Neoplasias: Mechanism, Regulation, And Perspectives, in: Molecular Cancer Research, 9, American Association for Cancer Research,, 2011, pp. 1435–1442, https://doi.org/10.1158/1541-7786.MCR-11-0154.

[5] S. Bhatia, S. Bhatia, Nanoparticles Types, Classification, Characterization, Fabrication Methods and Drug Delivery Applications. Natural Polymer Drug Delivery Systems, Springer International Publishing.,, 2016, pp. 33–93, https://doi.org/10.1007/978-3-319-41129-3_2.

[6] T. Birnbaum, E.A. Stadler, L. Baumgarten, Von, A. Straube, Rituximab significantly improves complete response rate in patients with primary CNS lymphoma, J. Neuro-Oncol. 109 (2) (2012) 285–291, https://doi.org/10.1007/s11060-012-0891-7.

[7] O. BP, D. PA, T. C, C. JR, The changing incidence of primary central nervous system lymphoma is driven primarily by the changing incidence in young and middle-aged men and differs from time trends in systemic diffuse large B-cell non-Hodgkin's lymphoma, Am. J. Hematol. 88 (12) (2013) 997–1000, https://doi.org/10.1002/AJH.23551.

[8] M. Çağdaş, A.D. Sezer, S. Bucak, Liposomes as Potential Drug Carrier Systems for Drug Delivery. Application of Nanotechnology in Drug Delivery, InTech,, 2014, https://doi.org/10.5772/58459.

[9] B.J. Chacko, S. Palanisamy, N.L. Gowrishankar, J. Honeypriya, A. Sumathy, Effect of surfactant coating on brain targeting polymeric nanoparticles; a review, Indian J. Pharm. Sci. 80 (2) (2018) 215–222, https://doi.org/10.4172/pharmaceutical-sciences.1000348.

[10] M. Danaei, M. Dehghankhold, S. Ataei, F. Hasanzadeh Davarani, R. Javanmard, A. Dokhani, S. Khorasani, M.R. Mozafari, Impact of particle size and polydispersity index on the clinical applications of lipidic nanocarrier systems, in: Pharmaceutics, Vol. 10, MDPI AG,, 2018, https://doi.org/10.3390/pharmaceutics10020057.

[11] R. Daneman, A. Prat, The blood–brain barrier, Cold Spring Harb. Perspect. Biol. 7 (1) (2015), https://doi.org/10.1101/cshperspect.a020412.

[12] E. Decaup, C. Jean, C. Laurent, P. Gravelle, S. Fruchon, F. Capilla, A. Marrot, T. Al Saati, F.X. Frenois, G. Laurent, C. Klein, N. Varoqueaux, A. Savina, J.J. Fournié, C. Bezombes, Anti-tumor activity of obinutuzumab and rituximab in a follicular lymphoma 3D model, Blood Cancer J. 3 (8) (2013) 131, https://doi.org/10.1038/bcj.2013.32.

[13] M. Gaumet, A. Vargas, R. Gurny, F. Delie, Nanoparticles for drug delivery: the need for precision in reporting particle size parameters, Eur. J. Pharm. Biopharm. 69 (1) (2008) 1–9, https://doi.org/10.1016/j.ejpb.2007.08.001.

[14] M. Gidwani, A. Singh, Nanoparticle enabled drug delivery across the blood brain barrier: in vivo and in vitro models, opportunities and challenges, Curr. Pharm. Biotechnol. 14 (14) (2014) 1201–1212, https://doi.org/10.2174/1389201015666140508122558.

[15] C. Grommes, L.M. Deangelis, Journal of clinical oncology primary CNS lymphoma, J. Clin. Oncol. 35 (2017) 2410–2418, https://doi.org/10.1200/JCO.2017.

[16] P.A. Klimiuk, I. Domysławska, Justyna Stanisław S., C. Chwiecko, Regulation of serum matrix metalloproteinases and tissue inhibitor of metalloproteinases-1 following rituximab therapy in patients with rheumatoid arthritis refractory to anti-tumor necrosis factor blockers, Rheuma Int 3 (2015) 749–755, https://doi.org/10.1007/s00296-014-3112-1.

[17] M. Koistinaho, S. Lin, X. Wu, M. Esterman, D. Koger, J. Hanson, R. Higgs, F. Liu, S. Malkani, K.R. Bales, S.M. Paul, Apolipoprotein E promotes astrocyte colocalization and degradation of deposited amyloid-β peptides, Nat. Med. 10 (7) (2004) 719–726, https://doi.org/10.1038/nm1058.

[18] J. Kreuter, Transport of drugs across the blood-brain barrier by nanoparticles, Curr. Med. Chem. -Cent. Nerv. Syst. Agents 2 (3) (2002) 241–249, https://doi.org/10.2174/1568015023357950.

[19] G.M. Kuesters, R.B. Campbell, Conjugation of bevacizumab to cationic liposomes enhances their tumor-targeting potential, Nanomedicine 5 (2) (2010) 181–192, https://doi.org/10.2217/nnm.09.105.

[20] U.H. Langen, S. Ayloo, C. Gu, Development and cell biology of the blood-brain barrier. In, in: Annual Review of Cell and Developmental Biology, Vol. 35, Annual Reviews Inc,, 2019, pp. 591–613, https://doi.org/10.1146/annurev-cellbio-100617-062608.

[21] M. Mrugala, A. Newcomer, T. Batchelor, Primary central nervous system lymphoma. Neurobiology of Disease, Elsevier Inc,, 2007, pp. 395–412, https://doi.org/10.1016/B978-012088592-3/50038-4.

[22] K. Nakamura, K. Yamashita, Y. Itoh, K. Yoshino, S. Nozawa, H. Kasukawa, Comparative studies of polyethylene glycol-modified liposomes prepared using different PEG-modification methods, Biochim. Et. Biophys. Acta - Biomembr. 1818 (11) (2012) 2801–2807, https://doi.org/10.1016/j.bbamem.2012.06.019.

[23] H.B. Newton, H.W. Slone, E.C. Bourekas, Primary central nervous system lymphoma. Handbook of Neuro-Oncology Neuroimaging: Second Edition, Elsevier Inc,, 2016, pp. 471–482, https://doi.org/10.1016/B978-0-12-800945-1.00041-0.

[24] P. Niparuck, P. Boonsakan, T. Sutthippingkiat, S. Pukiat, P. Chantrathammachart, S. Phusanti, K. Boonyawat, T. Puavilai, P. Angchaisuksiri, A. Ungkanont, S. Chuncharunee, V. Atichartakarn, Treatment outcome and prognostic factors in PCNSL, Diagn. Pathol. 14 (1) (2019) 56, https://doi.org/10.1186/s13000-019-0833-1.

[25] P.K. Pandey, A.K. Sharma, U. Gupta, Blood brain barrier: an overview on strategies in drug delivery, realistic in vitro modeling and in vivo live tracking. In, in: Tissue Barriers, Vol. 4, Taylor and Francis Inc,, 2016, https://doi.org/10.1080/21688370.2015.1129476.

[26] G.L. Plosker, D.P. Figgitt, Rituximab: a review of its use in non-hodgkin's lymphoma and chronic lymphocytic leukaemia. In, Drugs 63 (8) (2003) 803–843, https://doi.org/10.2165/00003495-200363080-00005.

[27] E.M. Rhea, W.A. Banks, Role of the Blood-Brain Barrier in Central Nervous System Insulin Resistance, in: Frontiers in Neuroscience, 13, Frontiers Media S.A., 2019, p. 521, https://doi.org/10.3389/fnins.2019.00521.

[28] J. Rip, Liposome technologies and drug delivery to the CNS. In, in: Drug Discovery Today: Technologies, 20, Elsevier Ltd,, 2016, pp. 53–58, https://doi.org/10.1016/j.ddtec.2016.07.005.

[29] J.L. Rubenstein, D. Combs, J. Rosenberg, A. Levy, M. McDermott, L. Damon, R. Ignoffo, K. Aldape, A. Shen, D. Lee, A. Grillo-Lopez, M.A. Shuman, Rituximab therapy for CNS lymphomas: targeting the leptomeningeal compartment, Blood 101 (2) (2003) 466–468, https://doi.org/10.1182/blood-2002-06-1636.

[30] S. Saesoo, S. Sathornsumetee, P. Anekwiang, C. Treetidnipa, P. Thuwajit, S. Bunthot, W. Maneeprakorn, L. Maurizi, H. Hofmann, R.U. Rungsardthong, N. Saengkrit, Characterization of liposome-containing SPIONs conjugated with

anti-CD20 developed as a novel theranostic agent for central nervous system lymphoma, Colloids Surf. B: Biointerfaces 161 (2018) 497–507, https://doi.org/10.1016/J.COLSURFB.2017.11.003.
[31] K. Sakata, M. Satoh, M. Someya, H. Asanuma, H. Nagakura, A. Oouchi, K. Nakata, K. Kogawa, K. Koito, M. Hareyama, T. Himi, Expression of matrix metalloproteinase 9 is a prognostic factor in patients with non-Hodgkin lymphoma, Cancer 100 (2004) 356–365.
[32] C.J. Schultz, J. Bovi, Current management of primary central nervous system lymphoma, Int. J. Radiat. Oncol. *Biol. *Phys. 76 (3) (2010) 666–678, https://doi.org/10.1016/J.IJROBP.2009.10.011.
[33] T. Siegal, O. Bairey, Primary CNS lymphoma in the elderly: the challenge, Acta Haematol. 141 (3) (2019) 138–145, https://doi.org/10.1159/000495284.
[34] E.V. Tchetina, A.N. Pivanova, G.A. Markova, G.V. Lukina, E.N. Aleksandrova, A. P. Aleksankin, S.A. Makarov, A.N. Kuzin, Rituximab downregulates gene expression associated with cell proliferation, survival, and proteolysis in the peripheral blood from rheumatoid arthritis patients: a link between high baseline autophagy-related ULK1 expression and improved pain control, Arthritis 2016 (2016) 1–12, https://doi.org/10.1155/2016/4963950.
[35] R.K. Upadhyay, Drug Deliv. Syst., CNS Prot., Blood Brain Barrier (2014), https://doi.org/10.1155/2014/869269.
[36] O. Veiseh, F.M. Kievit, R.G. Ellenbogen, M. Zhang, Cancer cell invasion: treatment and monitoring opportunities in nanomedicineer, in: Advanced Drug Delivery Reviews, 63, NIH Public Access,, 2011, pp. 582–596, https://doi.org/10.1016/j.addr.2011.01.010.
[37] L. Wang, W. Qin, Y.J. Huo, X. Li, Q. Shi, J.E.J. Rasko, A. Janin, W.L. Zhao, Advances in targeted therapy for malignant lymphoma, in: Signal Transduction and Targeted Therapy, 5, Springer Nature,, 2020, https://doi.org/10.1038/s41392-020-0113-2.
[38] K.C. Wu, S.T. Yang, T.C. Hsia, J.S. Yang, S.M. Chiou, C.C. Lu, R.S.C. Wu, J. G. Chung, Suppression of cell invasion and migration by propofol are involved in down-regulating matrix metalloproteinase-2 and p38 MAPK signaling in A549 human lung adenocarcinoma epithelial cells, Anticancer Res. 32 (11) (2012) 4833–4842. ⟨https://mdanderson.elsevierpure.com/en/publications/suppression-of-cell-invasion-and-migration-by-propofol-are-involv⟩.
[39] Y. Zhang, D. Zhou, Bin, P. Lyu, Primary central nervous system lymphoma: status and advances in diagnosis, molecular pathogenesis, and treatment. In, in: Chinese Medical Journal, 133, Lippincott Williams and Wilkins, 2020, pp. 1462–1469, https://doi.org/10.1097/CM9.0000000000000844.